

This article was downloaded by:

On: 21 January 2011

Access details: *Access Details: Free Access*

Publisher *Taylor & Francis*

Informa Ltd Registered in England and Wales Registered Number: 1072954 Registered office: Mortimer House, 37-41 Mortimer Street, London W1T 3JH, UK



## International Journal of Polymer Analysis and Characterization

Publication details, including instructions for authors and subscription information:

<http://www.informaworld.com/smpp/title~content=t713646643>

### X-Ray Photoelectron Spectroscopy and Atomic Force Microscopy of High-Solid Polyurethane Resins

Limin Wu<sup>a</sup>; Xichong Chen<sup>a</sup>; Lijun Zou<sup>a</sup>; Dongzhi Hu<sup>b</sup>

<sup>a</sup> Department of Materials Science, Fudan University, Shanghai, China <sup>b</sup> National Surface Physics Key Laboratory, Fudan University, Shanghai, China

Online publication date: 27 October 2010

**To cite this Article** Wu, Limin , Chen, Xichong , Zou, Lijun and Hu, Dongzhi(2003) 'X-Ray Photoelectron Spectroscopy and Atomic Force Microscopy of High-Solid Polyurethane Resins', *International Journal of Polymer Analysis and Characterization*, 8: 2, 83 – 98

**To link to this Article:** DOI: 10.1080/10236660304890

**URL:** <http://dx.doi.org/10.1080/10236660304890>

## PLEASE SCROLL DOWN FOR ARTICLE

Full terms and conditions of use: <http://www.informaworld.com/terms-and-conditions-of-access.pdf>

This article may be used for research, teaching and private study purposes. Any substantial or systematic reproduction, re-distribution, re-selling, loan or sub-licensing, systematic supply or distribution in any form to anyone is expressly forbidden.

The publisher does not give any warranty express or implied or make any representation that the contents will be complete or accurate or up to date. The accuracy of any instructions, formulae and drug doses should be independently verified with primary sources. The publisher shall not be liable for any loss, actions, claims, proceedings, demand or costs or damages whatsoever or howsoever caused arising directly or indirectly in connection with or arising out of the use of this material.

## ***X-Ray Photoelectron Spectroscopy and Atomic Force Microscopy of High-Solid Polyurethane Resins***

---

**Limin Wu, Xichong Chen, and Lijun Zou**

Department of Materials Science, Fudan University,  
Shanghai, China

**Dongzhi Hu**

National Surface Physics Key Laboratory,  
Fudan University, Shanghai, China

*High-solid polyester polyol resins and high-solid acrylic polyol resins were synthesized, cured by isophorone diisocyanate trimer (IPDI) to obtain polyurethane films, and then characterized by X-ray photoelectron spectroscopy (XPS) and atomic force microscopy (AFM). XPS analysis showed that the top layers of these polymer films are dominated by the soft segments of the resins; the IPDI segments tend to remain inside the bulk. The polyester resins cured by IPDI at room temperature show more soft segments than these resins cured by IPDI at 120°C. The change in mole ratios of hydroxyl to carboxylic and/or anhydride groups during the synthesis of the resins does not give rise to distinct variation in surface composition in our experimental range. AFM topographic images demonstrate that high-solid resins cured by IPDI exhibit numerous grains or aggregates on the surfaces, while low-solid resins cured by IPDI produce surfaces with only a few aggregates. Curing temperature, such as room temperature or 120°C, does not cause distinct differences in topographic images. Higher hydroxyl content of the resins results in smaller grains or aggregates on the surfaces. High-solid acrylic polyol resins cured by IPDI give rise to separated*

Received 10 November 2000; accepted 18 May 2001.

The authors are grateful to the Shanghai Dawn Foundation for financial support of this work.

Address correspondence to Limin Wu, Department of Materials Science, Fudan University, Shanghai 200433, China. E-mail: lxw@fudan.ac.cn

*aggregates surfaces, which is different from high-solid polyester polyol resins cured by IPDI.*

**Keywords:** High-solid; Polyester polyol resin; Acrylic polyol resin; XPS; AFM

The high-solid content resins are so called because less organic solvent is needed for them than for low-solid content resins. Because of increasingly strict solvent emission regulations in recent years, high-solid resins have become very desirable for use in coatings, adhesives, printing ink, electron sealants, and packaging materials instead of traditional resins, which usually need more organic solvent to obtain a given application viscosity. In general, low-molecular-weight and narrow-molecular-weight distribution are necessary to obtain low viscosity and high-solid resins. The lower the molecular weight, the lower the viscosity and the higher the solid content of the resin; the narrower the molecular weight distribution, the lower the viscosity and the higher the solid content of the resin. In other words, high molecular weight and wide molecular weight distribution always cause high viscosity and low-solid resins. In addition, each molecular chain must contain at least two functional groups for being cured by crosslinkers to obtain desirable film properties<sup>[1-4]</sup>. Therefore, for equal weight resins, the functionality content of high-solid-content resins is usually considerably more than that of the low-solid-content resins, which might result in different composition, structure, and properties.

X-ray photoelectron spectroscopy (XPS) has proved to be a very powerful tool for the characterization of the chemical composition of polymer surfaces up to several nanometers. Angle-dependent XPS analysis especially is of great value, not only revealing the different chemical compositions of polymer surfaces from their bulk, but also providing the depth profile of chemical composition, which has been extensively used for biopolymer, surface adhesion, durability, water- and grease-resistance of polymer films, etc.<sup>[5-9]</sup>

In addition to chemical characteristics of polymer surfaces obtained by XPS, physical orientation of the polymer surface could also be important in polymer characterization. Since its introduction in 1986<sup>[10]</sup>, atomic force microscopy (AFM) is one of the most successful tools in studying macromolecular surface science, such as surface topography and other physical properties<sup>[11-14]</sup>. Focused studies have been fruitful in revealing local adhesion, friction, mar resistance, shear, tribochemistry, etc., even down to the molecular and atomic scale<sup>[15-17]</sup>. The expansion of AFM technique is closely related to the strong demands for studying the surface properties at a nanometer scale. Progress has substantially improved our knowledge in many areas, correlating the structural characteristics with bulk properties.

In this study, we synthesized some low-molecular-weight, high-solid resins such as polyester polyol resins and acrylic polyol resins with various hydroxyl values, then cured these resins with polyisocyanate at room temperature or 120°C to obtain polyurethane films. We investigated the chemical composition and structure of the surfaces of these polymers from high-solid resins using XPS combined with AFM.

## EXPERIMENTAL

### Synthesis of High-Solid Polyester Polyol Resins

A 500-mL round-bottom flask equipped with a mechanical stirrer, a thermometer with a temperature controller, an N<sub>2</sub> inlet, a Graham condenser, and a heating mantle was charged with adipic acid, phthalic anhydride, neopentyl glycol, and 1,4-butanediol. The mole ratios of both adipic acid to phthalic anhydride and neopentyl glycol to 1,4-butanediol were kept constant while the mole ratios of hydroxyl to carboxylic and anhydride groups were varied and designated as PR-I, PR-II, PR-III, and PR-IV as described in Table I. When the flask was heated to around 120°C under a slow stream of N<sub>2</sub>, dibutyltin dilaurate of 0.05% based on all monomer weight was added as a catalyst. When the temperature was raised to 160°C, esterification reaction occurred and water began to distill out. The reaction was maintained at the desired temperature and time as shown in Table I, then cooled to room temperature and poured into a container. The hydroxyl numbers of

**TABLE I** The recipe for high-solid polyester resins

	PR-I	PR-II	PR-III	PR-IV
Adipic acid	72.12 g 0.494 mol	72.12 g 0.494 mol	72.12 g 0.494 mol	72.12 g 0.494 mol
Phthalic anhydride	14.8 g 0.1 mol	14.8 g 0.1 mol	14.8 g 0.1 mol	14.8 g 0.1 mol
Neopentyl glycol	14.10 g 0.135 mol	14.10 g 0.135 mol	12.27 g 0.118 mol	12.58 g 0.121 mol
1,4-butanediol	62.66 g 0.696 mol	62.66 g 0.696 mol	54.75 g 0.607 mol	56.1 g 0.622 mol
-OH/-COOH	1.4/1	1.4/1	1.22/1	1.25/1
Reaction condition	160° ~ 170°C, 4 h	200° ~ 210°C, 6 h	160° ~ 170°C, 4 h	160° ~ 170°C, 4 h

resins PR-I, PR-II, PR-III, and PR-IV are 123, 60, 80, and 96 mg KOH per gram polymer determined according to ASTM D1957-86, respectively. The polyester polyol resins were cured by IPDI for preparation for polyester-polyurethane films without further treatment.

### Synthesis of High-Solid Acrylic Polyol Resins

A 500-mL round-bottom flask equipped with a mechanical stirrer, a thermometer with a temperature controller, an N<sub>2</sub> inlet, a Graham condenser equipped with a cold finger using ice water as the cold trap, a dropping funnel, and a heating mantle was charged with half (15 g) of the total amount of 4-methyl-2-pentanone to be used and heated to 105°C. A solution of a mixture of 18.2 g of methyl methacrylate, 18.2 g of styrene, 48.4 g of butyl acrylate, 6.3 g or 18.9 g of 2-hydroxy ethyl methacrylate (HEMA), 6.1 g of 2-mercaptoethanol, 3.65 g of *t*-butyl peroxy 2-ethyl hexanoate (TBPH), and 15 g of 4-methyl-2-pentanone was added over a period of 1 h under a slow stream of N<sub>2</sub>. During the process of the addition of the monomer mixture, the temperature was maintained at 105 ± 2°C. When addition was complete, another 0.365 g of TBPH was added, and refluxing was continued for 1 h. The product was poured into a container and cooled to room temperature. The resins are designated as Acrylic I and Acrylic II when 6.3 g and 18.9 g of HEMA were used, respectively. The solid contents of Acrylic I and Acrylic II were measured at around 75% and 77% by ASTM D2369, respectively. The hydroxyl numbers of Acrylic I and Acrylic II were determined to be 70 and 110 mg KOH per gram polymer according to ASTM D1957-86, respectively.

### Preparation of Polyurethane Films

The solutions of these resins were combined with an isophorone diisocyanate trimer (IPDI) (solid content, 70%; NCO, 12%) using 1/1 weight ratio of resin to IPDI and adjusted to 70 wt.% solid content at application viscosity using 4-methyl-2-pentanone, leveling agent BYK320, and defoamer BYK070 (0.25 wt.% of the total weight of the resin and polyisocyanate on a solids basis) were prepared at room temperature in a 50-mL beaker. Just before application, dibutyltin dilaurate (0.05 wt.% of the total weight of the resin and polyisocyanate on total solids) was mixed thoroughly into the solution. Polyurethane films with a thickness of about 50 μm were prepared by casting the above solution on silicone panels using a drawdown rod. Some polyurethane films were dried at room temperature for 48 h, and others were baked at 120°C for 30 min.

## Characterization of Polyurethane Films

### XPS Measurement

Surface analyses of the polyurethane films were performed using XPS. The XPS experiments were conducted on a Kratos Analytical XSAM 800 pci X-ray photoelectron spectrometer located in Fudan's National Microanalysis Center. The system employs a non-monochromated Mg  $K_{\alpha}$  X-ray source. The X-ray gun was operated at 14 keV and 20 mA, and the system pressure was  $10^{-8}$  torr during analysis. Survey scans were taken over a binding energy range of 1150–0 eV to identify the elements on the top several nm of these polymer films based on the incident angle of photoelectron,  $60^{\circ}$  and  $90^{\circ}$ . Relative sensitivity factors for C, O, and N were derived from in-house standards. The uncertainty in reported atomic compositions are approximately  $\pm 5\%$  for C,  $\pm 10\%$  for O, and  $\pm 30\%$  for N. High-resolution  $C_{1s}$  spectra were acquired, and the contributions were resolved using a Gaussian-Lorentzian curve-fitting procedure using Kratoa vision software.

### AFM Measurement

AFM topographic images were obtained using a P47-SPM-MDT (Russia) with non-contact tapping mode and a resonant oscillating frequency of 463 kHz at ambient pressure, room temperature, and humidity. The quality of the applied commercial-etched silicon tips was checked before and after the measurements with a reference sample consisting of small round-shaped quantum dots. The mean spring constant of these tips was  $36 \text{ N m}^{-1}$ .

The mean surface roughness, which is the average vertical deviation of the surface relative to the center plane, and the root mean square were calculated by P47-SPM-MDT software from the follow equation

$$R_a = F(1, L_x, L_y) I\{0, L_y, I[0, L_x | f(x, y) | d_x] d_y\}$$

where  $f(x, y)$  is the surface relative to the center plane, and  $L_x$  and  $L_y$  are the dimensions of the surface. All the mean roughness values were averaged from several AFM images.

## RESULTS AND DISCUSSION

### Surface Chemical Composition of Polyurethane Films

The representative XPS spectrum is shown in Figure 1 for polyester-polyurethane film from PR-I resin cured by IPDI; the other resins cured by IPDI have the similar XPS spectra. The binding energies of  $C_{1s}$  are

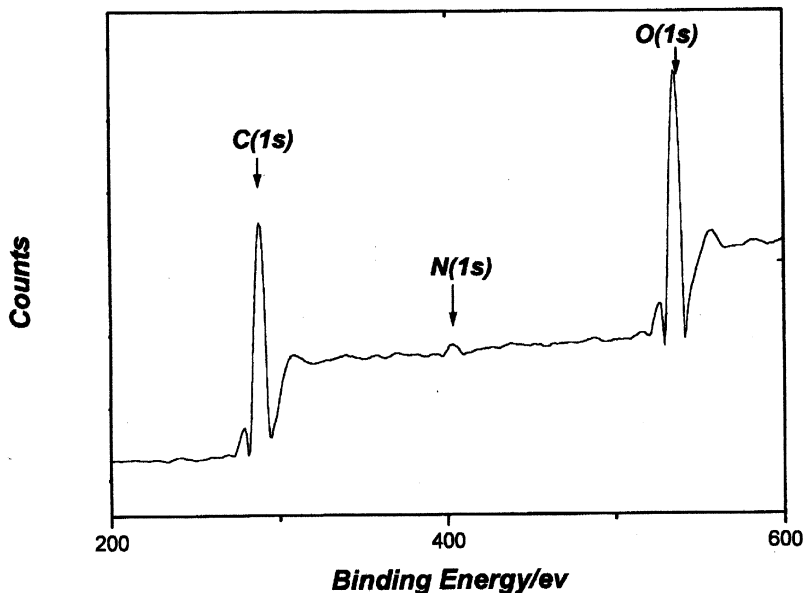
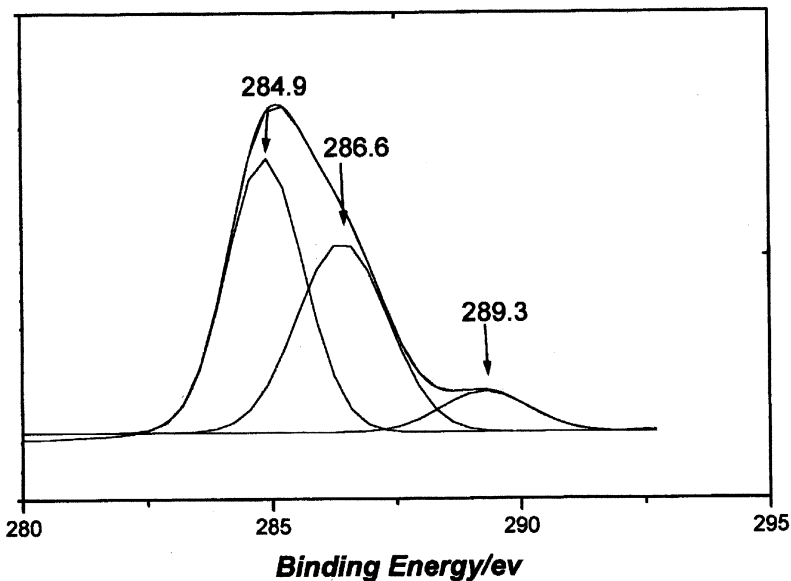


FIGURE 1 XPS survey scan of the polyurethane film from PR-I cured by IPDI.

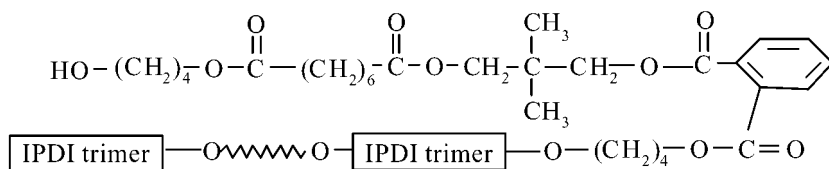
around (283–292 eV). The carbon peaks could be deconvoluted by curve fitting into three  $C_{1s}$  profiles as shown in Figure 2, with single core levels with assignments of 284.9 eV as aliphatic carbon or aromatic carbon ( $\underline{C}-C$ ,  $\underline{C}-H$ ), 286.6 eV as carbon bearing a single oxygen ( $\underline{C}-O$ ), and 289.3 eV as carboxylic carbon or urethane carbon ( $O-\underline{C}=O$ ,  $HN-\underline{C}=O$ ). The binding energies of  $O_{1s}$  and  $N_{1s}$  are around (534–540.0 eV) and 402.0 eV, respectively, corresponding to  $\pi$ -bonded oxygen ( $\underline{O}=\underline{C}$ ),  $\sigma$ -bonded oxygen ( $\underline{O}-C$ ), and  $\sigma$ -bonded nitrogen ( $\underline{N}-C$ ), respectively<sup>[18]</sup>.

The XPS data of polyester-polyurethane with the incident angles of  $60^\circ$  and  $90^\circ$  are summarized in Table II. Assuming only esterification reaction occurred during the process of synthesizing high-solid polyester polyol resins, and the addition reaction of hydroxy and isocyanate progressed when cured, the theoretical compositions for high-solid polyester polyol resins and the polyester-polyurethane films based on Table I and weight ratio of 1/1 of polyester resin to polyisocyanate are calculated in Table III. The comparison of Tables II and III illustrates that the concentrations of C and N atoms at the top layer of the polyester-polyurethane films are lower than their theoretical bulk composition while the concentration of O atoms is higher than their theoretical bulk composition, suggesting that the polyester-polyurethane films have a different composition between top layer and bulk, as was found in previous



**FIGURE 2** The deconvoluted spectrum of  $C_{1s}$  of the polyurethane film from PR-I cured by IPDI.

papers<sup>[9,19]</sup>. Since the theoretical composition of the polyester resins based on Table I are  $\sim 72$  and  $\sim 28$  for C and O atoms, respectively, while the theoretical composition of IPDI are 75.0%, 12.5%, and 12.5% for C, O, and N, respectively, the data in Table III show that the top layer is covered more by soft segments from the polyester resins, not the IPDI segments as shown in the schematic formula of polyester-polyurethanes:



Clearly, the segregation of these soft segments from polyester resins in the polyurethane films occurred. The principle driving force of this segregation is considered to be the interfacial free energy gap between the



**TABLE II** The XPS data for high-solid polyester resins cured by polyisocyanates

Samples and cure conditions	C(atom %)	O(atom %)	N(atom %)
PR-I room temperature			
60°	64.8	32.5	2.7
90°	67.2	28.2	4.6
PR-I 120°C			
60°	67.9	29.1	3.0
90°	69.3	26.3	4.4
PR-II room temperature			
60°	70.0	29.0	1.0
90°	70.1	27.2	2.7
PR-II 120°C			
60°	70.7	27.1	2.2
90°	71.0	25.0	4.0
PR-III room temperature			
60°	67.2	29.8	3.0
90°	67.7	28.0	4.3
PR-III 120°C			
60°	69.1	27.7	3.2
90°	71.4	26.1	4.5
PR-IV room temperature			
60°	67.1	30.3	2.6
90°	68.6	27.3	4.1
PR-IV 120°C			
60°	69.6	27.2	3.2
90°	70.3	25.0	4.7

initial and the final state. Generally, the surfaces of samples of the block copolymers themselves, as well as mixtures containing them, are substantially enriched in the component of lower surface energy, as described for other block copolymers or blends, such as PS-PEO and PEO-PPO copolymers<sup>[7]</sup> and PS-PDMS copolymer<sup>[20]</sup>. Using the surface free energies of poly(tetramethylene oxide) segments and 4,4'-diphenylmethane diisocyanate segments, which are analogous to our soft segments and IPDI segments in structure, respectively, having surface free energies of  $\sim 32$  dyn/cm and  $\sim 49$  dyn/cm, respectively<sup>[21]</sup>, the soft segments from the polyester resins should have lower surface free energy than IPDI segments in polyurethanes. Thus, the soft segments from the polyester resins tend to cover the top layer to maintain the minimum energy state while the IPDI segments tend to retain in bulk because of their high surface free energy and cyclic trimer structure. The concentration of O atoms decreases and the concentration of N atoms increases with larger incident

**TABLE III** The theoretical compositions for high-solid polyester resins and polyurethane films

	C(atom %)	O(atom %)	N(atom %)
PR-I resin cured by IPDI	73.1	21.7	5.2
PR-II resin cured by IPDI	73.1	21.7	5.2
PR-III resin cured by IPDI	73.3	21.5	5.2
PR-IV resin cured by IPDI	73.2	21.5	5.3
PR-I resin	71.7	28.3	–
PR-II resin	71.7	28.3	–
PR-III resin	72.0	28.0	–
PR-IV resin	71.9	28.1	–
IPDI	75.0	12.5	12.5
Neopentyl glycol	71.4	28.6	–
1,4-butanediol	66.7	33.3	–

angle ( $60^\circ$  and  $90^\circ$ ) as we go deeper into the top layer. These results suggest that the soft segments of polyester resins tend to cover the top surface and the IPDI segments tend to remain inside the bulk; the composition of the top layer varies stepwise with depth profile.

The comparison of polyester resins cured by IPDI at room temperature with those cured at  $120^\circ\text{C}$  illustrates that curing at room temperature causes much fewer C and N atoms and more O atoms at the top layer than curing at  $120^\circ\text{C}$ , as shown in Table II. Recall that the excess diols were always used for synthesizing high-solid polyester resins in our experiments. This means that some residual diols or their derivatives from these diols also exist in these polyester resins. When cured at  $120^\circ\text{C}$ , these residual diols plus polyester polyol resins are fully cross-linked with polyisocyanate through the reaction of -OH and -NCO groups. But when cured at room temperature, not every diol molecule causes a cross-linking reaction with polyisocyanate; the free diols without being reacted with polyisocyanate move toward the top layer. Since the C atomic numbers are lower and O atomic numbers of the residual diols are higher than for polyester resins and IPDI, especially for 1,4-butanediol as indicated in Table III, this movement of the residual diols toward the surface results in lower concentration of C and N atoms and higher O atom concentration than resin cured at  $120^\circ\text{C}$ . The change in mole ratios of hydroxyl to carboxylic and anhydride groups during the synthesis does not cause distinct variation in surface composition in our experimental range. Extending esterification reaction and raising reaction temperature lead to a polyester with higher molecular weight and lower residual diol monomer concentration based on step polymerization mechanism,

causing higher C atomic concentration and lower O atomic concentration, as seen in Table II comparing PR-II and PR-I.

## AFM Analysis of Polymer Films

The AFM topographic images of some high-solid polyester resins cured by IPDI at room temperature and 120°C and of high-solid acrylic resins with different hydroxyl values cured by IPDI at room temperature are presented in Figures 3 through 6. AFM offers the advantages of high resolution, especially in the vertical direction, which is difficult to obtain with conventional electron microscopy, along with relative ease of sample preparation. When cured at room temperature, the polyurethane film from PR-I and IPDI has a rough surface composed of numerous grains or aggregates (Figure 3a). The surface roughness  $R_a$  (average vertical deviation about the mean plane) is 0.275, obtained by averaging measurements for several images of polyurethane film made of PR-I resin and IPDI. Another common surface roughness parameter, the root mean square (rms) is 0.347 as indicated in Table IV. The lateral size ( $x, y$ ) of the grains or aggregates is 40–150 nm, and the maximum peak height  $Z_{\max}$  is  $\sim 3$  nm. When cured at 120°C, the polymer film has a relatively smooth surface composed of numerous small grains (Figure 3b). The mean roughness and the root mean square of the surface are 0.184 and 0.232, respectively. The lateral size ( $x, y$ ) of the grains is 30–90 nm, and the maximum peak height  $Z_{\max}$  is  $\sim 1.7$  nm.

The polyurethane films from the PR-II resin cured by IPDI show only a few polymer aggregates on the surface with a scan area of  $2 \times 2 \mu\text{m}$  that are relatively smooth for both film cured at room temperature and film cured at 120°C as seen in Figure 4a and 4b, respectively. The surface roughness parameters are listed in Table IV. Recall that the PR-II resin was obtained by esterification at higher reaction temperature (200°C–210°C) and much longer reaction time (6 h) than PR-I resin, although both had the same monomers recipes. In other words, PR-II resins have properties much closer to those of the traditional low-solid polyester resin, e.g., high molecular weight and low functionality content. Thus, we can say that high-solid resins show more grains or aggregates on their surfaces than low-solid resins, or that these grains or aggregates are related to the molecules with low molecular weight<sup>[18]</sup>.

The topographic images of polyurethane films from PR-III cured by IPDI further support this point. The polyurethane film from PR-III cured by IPDI has a rough surface consisting of some aggregates when cured at room temperature (Figure 5a); the  $R_a$  and rms are 0.187 and 0.233, respectively. The lateral size ( $x, y$ ) of the aggregates is  $\sim 50$ –450 nm, and the maximum peak height is  $\sim 1.4$  nm. When cured at 120°C, the polyurethane film has a similar rough surface consisting of aggregates, but

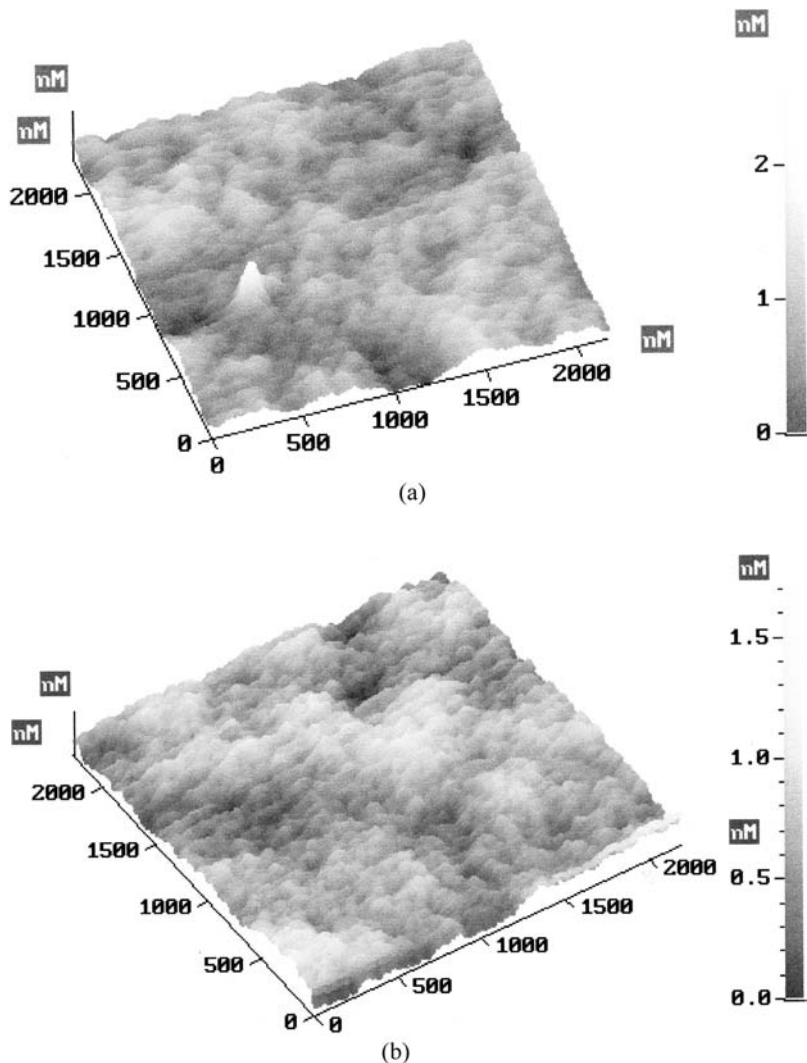


**FIGURE 3** AFM topographic images of the polyurethane film from PR-I cured by IPDI. (a) At room temperature; (b) 120°C.

some packed grains can be observed (Figure 5b). The  $R_a$  and rms are 0.199 and 0.254, respectively. The lateral size (x, y) of the aggregates is ~50–400 nm, and the maximum peak height is ~1.8 nm. Comparison of the AFM topographic images between the polymer films from PR-I cured

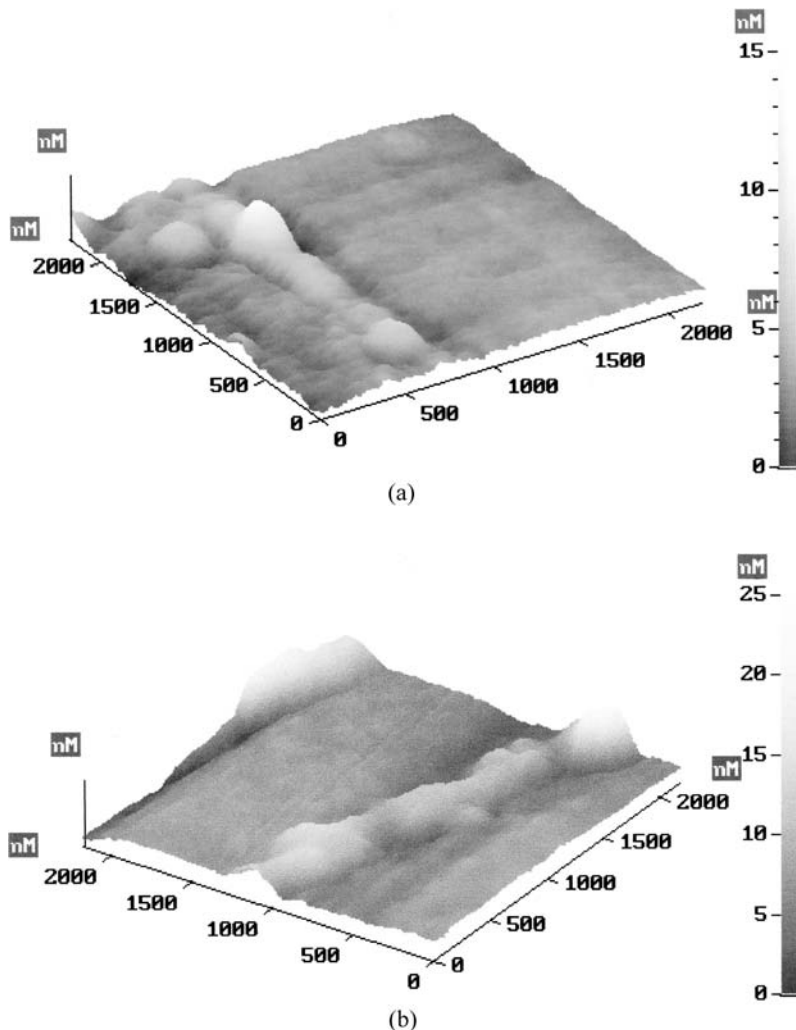


**FIGURE 4** AFM topographic images of the polyurethane film from PR-II cured by IPDI. (a) At room temperature; (b) 120°C.

with IPDI and PR-III cured with IPDI is very interesting: The polymer films from PR-I and IPDI usually contain a lot of grains while those from PR-III cured with IPDI usually contain some aggregates. Recall that the mole ratios of hydroxyl to carboxylic and anhydride groups are 1.4/1 for PR-I resin and 1.22/1 for PR-III resin, respectively. The different surface

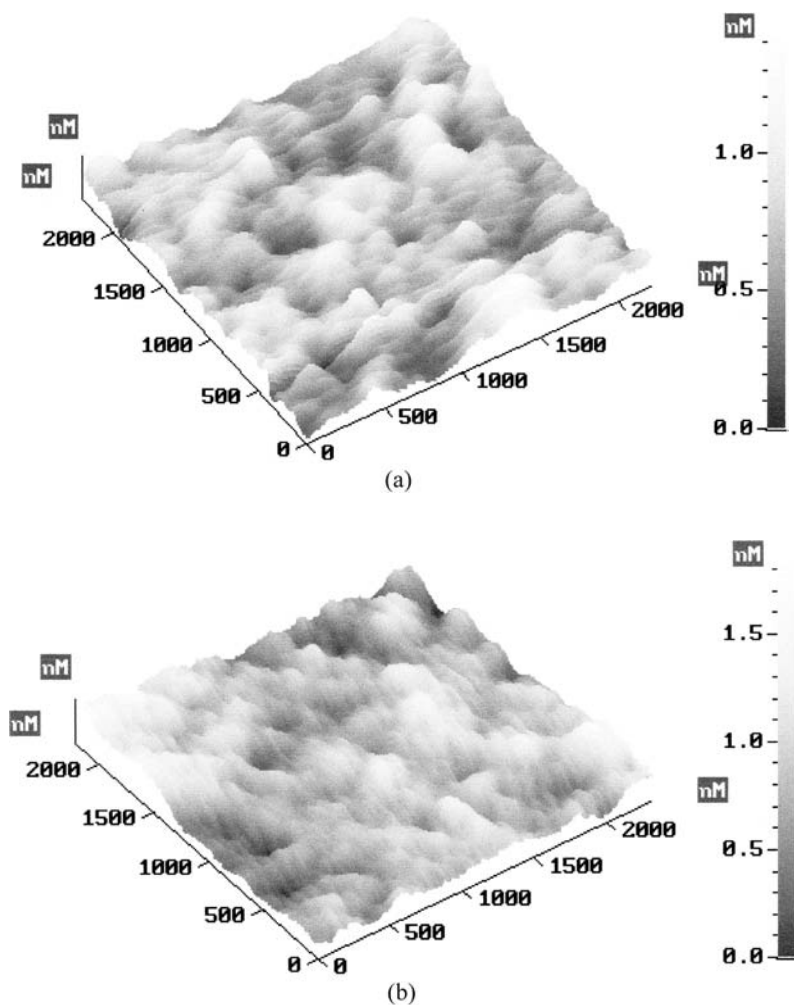


**FIGURE 5** AFM topographic images of the polyurethane film from PR-III cured by IPDI. (a) At room temperature; (b) 120°C.

structures suggest that the more the diols, the lower the molecular weight, resulting in more grains on the surface.

Further, we synthesized two high-solid acrylic polyol resins—Acrylic I and Acrylic II, with hydroxyl values of 70 and 110, respectively—and cured these two acrylic polyol resins using IPDI at room temperature based on a weight ratio of 1/1 and observed their AFM topographic images as shown in

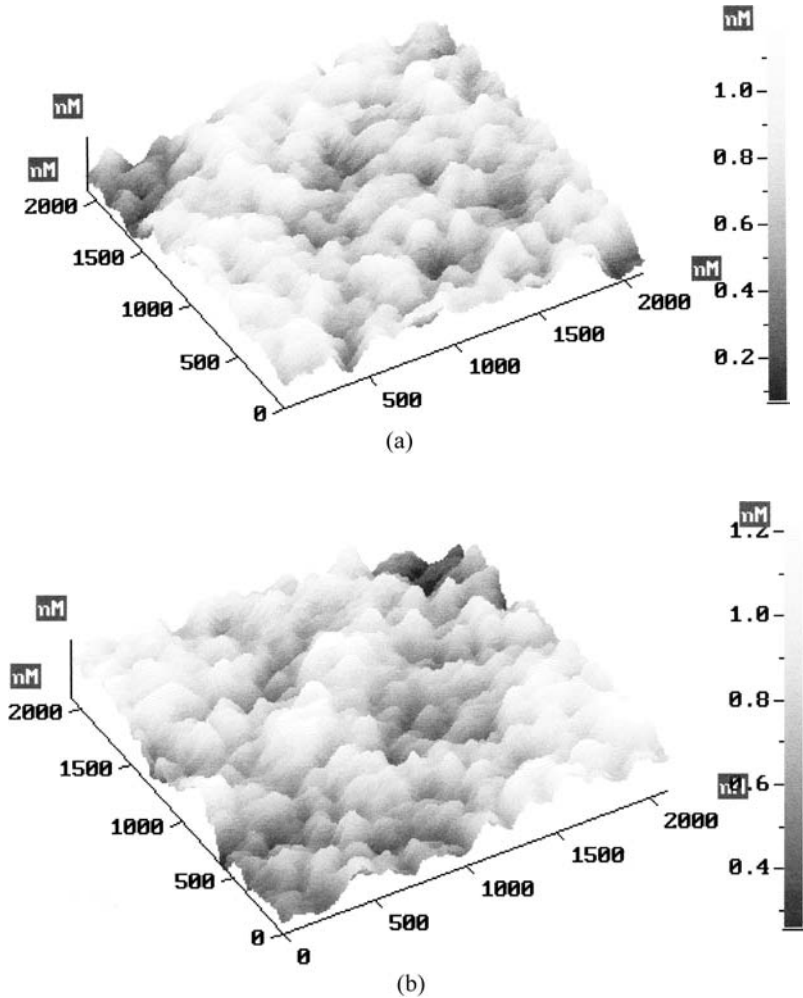


**FIGURE 6** AFM topographic images of the polyurethane film from acrylic resins cured by IPDI at room temperature. (a) Acrylic I; (b) Acrylic II.

Figure 6. The polymer film from Acrylic I cured by IPDI has larger aggregates on the surface (Figure 6a) than the film from Acrylic II cured by IPDI (Figure 6b). The  $R_a$  and rms of the polymer film from Acrylic I cured by IPDI are 0.177 and 0.223, respectively; the aggregate has a size of  $\sim 50$ – $450$  nm, and the maximum peak height is  $\sim 1.2$  nm. The  $R_a$  and rms of the polymer film from Acrylic II cured by IPDI are 0.171 and 0.212,

**TABLE IV** Mean roughness and root mean square of polymer films

	PR-I cured by IPDI		PR-II cured by IPDI		PR-III cured by IPDI		Acrylic I 70	Acrylic II 110
	RT <sup>a</sup>	120°C	RT	120°C	RT	120°C	RT	RT
R <sub>a</sub>	0.275	0.184	0.841	1.61	0.187	0.199	0.177	0.171
rms	0.347	0.232	1.37	2.41	0.233	0.254	0.223	0.212

<sup>a</sup>Room temperature.

respectively; the aggregate has a size of ~50–410 nm, and the maximum peak height is ~1.2 nm. Again, the low molecular weight, high-solid resins cause the surfaces with numerous aggregates or grains compared with high-molecular-weight, low-solid resins. Meanwhile, the surface structure of high-solid acrylic resins cured by IPDI is considerably different from that of high-solid polyester resins cured by IPDI. For high-solid acrylic resins cured by IPDI, there is a distinct separation between aggregates, but for high-solid polyester resins cured by IPDI, the grains or aggregates are not obviously separated from each other.

## CONCLUSION

High-solid polyester resins and acrylic resins were synthesized and cured by IPDI, and then characterized by XPS and AFM. XPS analysis shows that the composition of the top layers of these polymer films are different than their bulk composition: The top layers are dominated by soft segments of the resins, and the IPDI segments tend to remain inside the bulk. The polyester resins cured by IPDI at room temperature show lower concentration of C and N atoms and higher O atomic concentration than the same polyester resins cured by IPDI at 120°C, indicating that the former have more soft segments than the latter because of residual diol monomers and their derivatives. The change in mole ratios of hydroxyl groups to carboxylic and anhydride groups during synthesis does not cause distinct variation in surface composition in our experimental range.

AFM topographic images demonstrate that high-solid resins cured by IPDI cause numerous grains or aggregates to appear on the surface, while low-solid resins cured by IPDI produce surfaces with only a few aggregates. Curing conditions, such as room temperature or 120°C, do not cause a distinct difference in topographic image. With higher hydroxyl content of the resins, the lower the molecular weight, resulting in more



grains on the surface. High-solid acrylic polyol resins cured by IPDI cause separated aggregates or grains on the surfaces while high-solid polyester polyol resins cured by IPDI do not produce distinct separated grains on the surfaces.

## REFERENCES

- [1] Wicks, Z. W., Jr., F. N. Jones, and S. P. Pappas. (1999). *Organic Coatings: Science and Technology*. 2nd ed., p. 21. New York: Wiley-Interscience.
- [2] Hawker, C. J., E. Elce, J. Dao, W. Volksen, T. P. Russell, and G. G. Barclay. (1996). *Macromolecules*. 29:2686.
- [3] Wang, J. L., T. Grimaud, and K. Matyjaszewski. (1997). *Macromolecules*. 30:6507.
- [4] U.S. Patent 5,976,706. (1999).
- [5] Graham, S. W. and D. M. Hercules. (1981). *J. Biomed. Mater. Res.* 15:349.
- [6] Bummer, P. M. and K. Knutson. (1990). *Macromolecules*. 23:4357.
- [7] Gaines, G. L., Jr. (1981). *Macromolecules*. 14:208.
- [8] Wu, L., D. M. Weisberg, J. Runt, G. Felder III, A. J. Snyder, and G. J. Rosenberg. (1999). *J. Biomed. Mater. Res.* 44:371.
- [9] Wu, L., D. Li, B. You, and F. Qian. (2000). *Int. J. Polym. Anal. Charact.* 5:491.
- [10] Binnig, G., C. F. Quate, and C. Gerber. (1986). *Phys. Rev. Lett.* 56:9309.
- [11] Snetivy, D. and G. J. Vancso. (1994). *Polymer*. 35:461.
- [12] Goh, M. C., D. Juhue, G. Wang, Q. M. Leung, and M. A. Winnik. (1993). *Langmuir*. 9:1319.
- [13] Magonov, S. N., K. Quarnstrom, V. Elings, and H.-J. Cantow. (1991). *Polym. Bull.* 25:689.
- [14] Albrecht, T. R., M. M. Dovek, C. A. Lang, P. Grutter, C. F. Quate, S. W. J. Kuan, C. W. Frank, and R. F. W. Pease. (1988). *J. Appl. Phys.* 64(3):1178.
- [15] Idla, K., A. Talo, H. E.-M. Niemi, O. Forsén, and S. Yläsaari. (1997). *Surf. Interface Anal.* 25:837.
- [16] Bai, C., J. Li, Z. Lin, J. Tang, and C. Wang. (1999). *Surf. Interface Anal.* 28:44.
- [17] Uchida, E., H. Iwata, and Y. Ikada. (2000). *Polymer*. 41:3609.
- [18] Teare, D. O. H., C. Ton-That, and R. H. Brandley. (2000). *Surf. Interface Anal.* 29:276.
- [19] Sung, C. S. P. and N. S. Schneider. (1977). *Macromolecules*. 10:452.
- [20] Gaines, G. L., Jr. and G. W. Bender. (1972). *Macromolecules*. 5:82.
- [21] Wu, S. (1989). In *Surface and Interfacial Tensions of Polymers, Oligomers, Plasticizers and Organic Pigments in Polymer Handbook*, ed. J. Brandrup and E. H. Immerguy. 3d ed; pp. vi, 411–428. New York: John Wiley.